Eur. Phys. J. C 42, 127–137 (2005)
Digital Object Identifier (DOI) 10.1140/epjc/s2005-02253-6

THE EUROPEAN PHYSICAL JOURNAL C

Classical solutions in a Lorentz violating scenario of Maxwell–Chern–Simons–Proca electrodynamics

H. Belich Jr.[1,a], T. Costa-Soares[2,4,b], M.M. Ferreira Jr.[3,c], J.A. Helayël-Neto[4,d]

[1] Universidade Federal do Espírito Santo (UFES), Departamento de Física e Química, Av. Fernando Ferrari, S/N Goiabeiras, Vitória – ES, 29060-900 – Brasil
[2] Universidade Federal de Juiz de Fora (UFJF), Colégio Técnico Universitário, av. Bernardo Mascarenhas, 1283, Bairro Fábrica – Juiz de Fora – MG, 36080-001 – Brasil
[3] Universidade Federal do Maranhão (UFMA), Departamento de Física, Campus Universitário do Bacanga, São Luiz – MA, 65085-580 – Brasil
[4] CBPF - Centro Brasileiro de Pesquisas Físicas, Rua Xavier Sigaud, 150, CEP 22290-180, Rio de Janeiro, RJ, Brasil

Received: 24 February 2005 / Revised version: 12 April 2005 /
Published online: 31 May 2005 –

Abstract. Taking as starting point the planar model that arises from the dimensional reduction of the Abelian-Higgs Carroll–Field–Jackiw model, we write down and study the extended Maxwell equations and the associated wave equations for the potentials. The solutions for these equations correspond to the usual ones for the MCS-Proca system, supplemented with background-dependent correction terms. In the case of a purely timelike background, exact algebraic solutions are presented which possess a similar behavior to the MCS-Proca counterparts near and far from the origin. On the other hand, for a purely spacelike background, only approximate solutions are feasible. They consist of non-trivial analytic expressions with manifest evidence of spatial anisotropy, which is consistent with the existence of a privileged direction in space. These solutions also behave similarly to the MCS-Proca ones near and far from the origin.

PACS. 11.10.Kk, 11.30.Cp, 11.30.Er

1 Introduction

Lorentz and CPT violating theories in $(1+3)$ dimensions have been object of intensive investigation in the latest years [1–12]. An odd-CPT Lorentz violating model (with a Chern–Simons-like term) was considered in a pioneering work in the context of classical electrodynamics by Carroll–Field–Jackiw [1], by setting up a simple way to realize the CPT and Lorentz breaking in the framework of the Maxwell theory. In a general perspective, an extension of the minimal $SU(3) \times SU(2) \times U(1)$ standard model incorporating odd- and even-CTP terms was developed by Colladay and Kostelecky [2] as a low-energy limit of a Lorentz covariant model valid at the Planck scale. This master model undergoes a spontaneous symmetry breaking, generating an effective action that incorporates Lorentz violation and keeps unaffected the $SU(3) \times SU(2) \times U(1)$ gauge structure and the energy-momentum conservation. This standard model extension (SME) has then been investigated under diverse aspects [4,6].

The Carroll–Field–Jackiw model[1], in spite of predicting several interesting new properties and a potentially rich phenomenology, is a model plagued with some serious problems, like the absence of stability and causality in the case of a purely timelike background, $v^\mu = (v_0, 0)$. Even so, this theory has been fairly well discussed under a number of different aspects, like the following ones:
(i) the birefringence (optical activity of the vacuum), induced by the fixed background [1,7],
(ii) the investigation of radiative corrections [8],
(iii) the consideration of spontaneous breaking of $U(1)$-symmetry in this framework [9],
(iv) the search for a supersymmetric Lorentz violating extension model [10],
(v) the study of vacuum Cerenkov radiation [11], the photon decay process [12], and some other points.

The great interest aroused by such an issue has motivated the study of Lorentz violating theories in lower dimensions. In this sense, a dimensional reduction (to $D = 1 + 2$) of the Lorentz breaking Maxwell electrodynamics, endowed with the Carroll–Field–Jackiw term $(\epsilon^{\mu\nu\kappa\lambda} v_\mu A_\nu F_{\kappa\lambda})$ [1], has been recently performed [13],

[a] e-mail: belich@cce.ufes.br
[b] e-mail: tcsoares@cbpf.br
[c] e-mail: manojr@ufma.br
[d] e-mail: helayel@cbpf.br

yielding a gauge invariant planar quantum electrodynamics (QED_3) composed of a Maxwell–Chern–Simons gauge sector, a Klein–Gordon massless scalar field (φ), and the fixed 3-vector (v^μ), responsible for the Lorentz violation. As for the physical consistency of this model, some of its general features have been investigated. One has then verified that the complete model is stable and preserves causality and unitarity without any restrictions [13]. Therefore, the full model supports a consistent quantization for both time- and spacelike backgrounds. Furthermore, the classical equations of motion and solutions of this Lorentz violating planar model were considered as well [14], revealing interesting deviations in relation to the pure MCS case, like the absence of screening in the electric sector for a purely timelike background and manifest anisotropy for a purely spacelike background.

The Carroll–Field–Jackiw model has been also considered in the context of a $U(1)$ spontaneous symmetry breaking, yielding an Abelian–Higgs Lorentz violating model in (1+3) dimensions endowed with stable vortex configurations [9]. In a further work [15], one has carried out the dimensional reduction of this master model to (1+2) dimensions, obtaining a planar Lorentz violating Lagrangian with the Higgs sector. The consistency of this model was properly analyzed at the classical level, revealing preservation of causality, stability and unitarity for both time- and spacelike backgrounds, in a similar way to the case addressed in [13]. Recently, one has also investigated the presence of vortex configurations in this planar framework [16], and it has been found out that there may appear stable configurations of electrically charged vortices which induce an Aharonov–Casher phase for neutral particles.

To study Lorentz violating theories, we have adopted a general procedure that consists in investigating and setting up its classical aspects before addressing the second-quantized case. With this program in mind, we have discussed the consistency (causality, unitarity and stability) of the Higgs–Carroll–Field–Jackiw model both in $(1+3)$ and $(1+2)$ dimensions, based on the dispersion relations that are read off as poles of the propagators. This task may indeed indicate the eventual presence of non-physical modes, such as spacelike poles (tachyons) and negative-norm 1-particle states (ghosts). Once one has thereby fixed the parameters of the model and selected the situations for which the spectrum does not display unphysical excitations, it is sensible to carry out the second quantization of the system.

In the present paper, one follows this general procedure, now focusing the attention on the classical electrodynamics that stems from the $U(1)$ broken phase of the planar version of the Abelian–Higgs CFJ model. The main goal is to describe the influence of the Lorentz violating background on the solutions associated with a system of point-like charges, bearing in mind the results obtained in [14], which revealed the possibility of having new physics induced by the presence of the background (as the vanishing of the screening associated with the MCS electrodynamics, for instance). In this sense, one first writes down the tree-level Lagrangian of the $U(1)$ broken phase of the Higgs–Abelian model worked out in [15]; it is composed of a MCS-Proca gauge sector coupled to a Klein–Gordon massive field by means of the Lorentz violating term. The associated classical equations of motion (the extended Maxwell equations) and wave equations (for the potential A^μ) are written in the sequel. Such equations correspond to the ones of the usual MCS-Proca electrodynamics supplemented by terms that depend on the background vector. So, it might be expected that the solutions we find correspond to the MCS-Proca ones corrected by background-dependent terms. Indeed, this is the case. Proceeding further, solutions for field strengths and potentials have been found for point-like charges (both for purely timelike and spacelike backgrounds), exhibiting v^μ-dependent corrections with respect to the pure MCS-Proca counterparts.

Specifically, in the case of a purely timelike background, exact algebraic solutions are attained by means of Fourier integrations. Both the scalar and vector potentials are given in terms of linear combinations of modified Bessel functions (K_0, K_1) and behave at the origin and far from it in much the same way as the pure MCS-Proca solutions; the difference always occurs at some intermediary radial region. Since these Bessel functions decay exponentially, it is evident that the associated solutions present a strong screening, typical for the case where the physical intermediation is played only by massive particles. It has also been noticed that the scalar potential (A_0) exhibits a familiar form, similar to the MCS-Proca solution. However, it may significantly differ from the latter potential in the case of a small Proca mass $(M_A/s \ll 1)$ or a large background $(v_0 \lesssim s)$, in which case it becomes attractive in some radial range. As for the vector potential $(\mathbf{A})$, one is able to write down a solution rather similar to the MCS-Proca counterpart, without qualitative alterations. However, these solutions may differ substantially at intermediary distances for the case in which $(v_0 \lesssim s)$. Plots are introduced to illustrate the points alluded to here.

On the other hand, in the case of a purely spacelike background, the Fourier integrations as a result are no more exactly soluble, implying the necessity of employing approximations which lead to algebraic solutions of great complexity (in leading order in v^2/s^2). The presence of spatial anisotropy becomes a manifest property, in the form of correction terms with a clear dependence on the angle determined by the fixed background $(\boldsymbol{v})$. The scalar potential worked out consists of a complex combination of Bessel and radial functions $(K_0, rK_1, K_1/r)$; its forms near and far from the origin are qualitatively similar to the MCS-Proca case: it vanishes for $r \to \infty$ and goes as $\ln r$ for $r \to 0$. Concerning the vector potential, it also appears as a lengthy combination of Bessel and radial functions $(rK_0, K_0/r, K_1, K_1/r^2)$, exhibiting anisotropy terms. In spite of the involved complexity, this potential presents an identical behavior to the MCS-Proca counterpart near and away from the origin. A graphical analysis reveals that the presence of the background does not amount to qualitative or sensitive modifications on the MCS-Proca solutions, be-

cause of the small magnitude of the background compared with the Chern–Simons parameters ($v^2/s^2 \ll 1$).

The method of investigation adopted here has yielded solutions for the Klein–Gordon field as well, revealing an analogous structure to the scalar potential both in the purely timelike and spacelike backgrounds. Moreover, it is important to point out that such solutions recover the pure MCS-Proca results in limit of a vanishing background ($v^\mu = 0$), which is a necessary condition to attest the validity of the solutions found out.

In short, this paper is outlined as follows. In Sect. 2, we present the basic features of the reduced model, previously developed in [15]. In Sect. 3, the equations of motion, from which one derives the wave equations for potentials and field strengths, are presented. In Sect. 4, we solve the equations for the scalar potential (in the static limit) for the time- and spacelike cases and discuss the results. In Sect. 5, we solve the differential equations for the vector potential according to the procedure adopted in Sect. 4. In Sect. 6, we present our conclusions and make some final remarks.

2 The dimensionally reduced Lorentz violating model

We take as starting point the Carroll–Field–Jackiw Lorentz violating electrodynamics minimally coupled to a scalar field sector, endowed with spontaneous symmetry breaking [9][1]:

$$\mathcal{L}_{1+3} = -\frac{1}{4}F_{\hat{\mu}\hat{\nu}}F^{\hat{\mu}\hat{\nu}} + \frac{1}{4}\varepsilon^{\hat{\mu}\hat{\nu}\hat{\kappa}\hat{\lambda}}v_{\hat{\mu}}A_{\hat{\nu}}F_{\hat{\kappa}\hat{\lambda}} + (D^{\hat{\mu}}\phi)^* D_{\hat{\mu}}\phi - V(\phi^*\phi) - A_{\hat{\nu}}J^{\hat{\nu}}, \quad (1)$$

where $v^{\hat{\mu}}$ stands for the fixed background (associated with the Lorentz violation at the level of the particle frame) [3] and the Greek letters with hat, $\hat{\mu}$, run from 0 to 3. Here, $D_{\hat{\mu}} = (\partial_{\hat{\mu}} + \mathrm{i}eA_{\hat{\mu}})$ is the covariant derivative which sets up the minimal coupling with the scalar field while $V(\phi^*\phi) = m^2\phi^*\phi + \lambda(\phi^*\phi)^2$ represents the scalar potential responsible for spontaneous symmetry breaking. The theoretical model of the Lagrangian (1) was analyzed in [9], in which it has been shown that it is consistent (endowed with causality and unitarity) only for a purely timelike background.

We should now consider the dimensionally reduced version of this model, which has been developed and analyzed in [15], where one can find the motivations to consider it and details of the reduction process are given. Applying the prescription of the dimensional reduction, described in [13,15], on (1), one obtains the reduced planar Lagrangian:

$$\mathcal{L}_{1+2} = -\frac{1}{4}F_{\mu\nu}F^{\mu\nu} + \frac{1}{2}\partial_\mu\varphi\partial^\mu\varphi + \frac{s}{2}\epsilon_{\mu\nu k}A^\mu\partial^\nu A^k - \varphi\epsilon_{\mu\nu k}v^\mu\partial^\nu A^k + (D_\mu\phi)^*(D_\mu\phi) - e^2\varphi^2(\phi^*\phi) - V(\phi^*\phi) - A_\mu J^\mu - \varphi J, \quad (2)$$

where the Greek letters (now without hat) run from 0 to 2. The scalar field, φ, is the remanent of the compactified coordinate of the vector potential ($A^{(3)} = \varphi$), here acting as a massless Klein–Gordon field. The mixing Chern–Simons-like term, $\varphi\epsilon_{\mu\nu k}v^\mu\partial^\nu A^k$, in spite of being covariant in form, is not Lorentz invariant in the particle frame, in which the fixed (v^μ) background does not boost as a 3-vector. The Lagrangian (2) represents a field model endowed with Lorentz violation and spontaneous symmetry breaking, which may constitute a theoretical framework useful to analyze planar vortex configurations. Its components present the following mass dimension: $[A^\mu] = [\varphi] = 1/2$, $[s] = [v^\mu] = 1$, $[J^\mu] = 5/2$.

Having established the planar Lorentz violating model, we can now consider the spontaneous symmetry breaking process, which provides mass to the gauge and scalar fields [15]. Once we are bound to a tree-level analysis, we then retain only the bilinear terms, so that the planar Lagrangian takes the form

$$\mathcal{L}^{\text{broken}}_{1+2} = -\frac{1}{4}F_{\mu\nu}F^{\mu\nu} + \frac{1}{2}\partial_\mu\varphi\partial^\mu\varphi - \frac{1}{2}M_A^2\varphi^2 + \frac{s}{2}\epsilon_{\mu\nu k}A^\mu\partial^\nu A^k - \varphi\epsilon_{\mu\nu k}v^\mu\partial^\nu A^k + \frac{1}{2}M_A^2A_\mu A^\mu - A_\mu J^\mu - \varphi J, \quad (3)$$

where $M_A^2 = 2e^2\langle\phi\phi\rangle$, with $\langle\phi\phi\rangle$ being the vacuum expectation value of the scalar field. The tree-level Lagrangian above represents a theoretical model composed of a Maxwell–Chern–Simons–Proca gauge sector, the massive Klein–Gordon field and the Lorentz violating mixing term. This is the Maxwell–Chern–Simons–Proca electrodynamics corrected by the presence of the fixed background. The Higgs field is not considered in the Lagrangian above once we work in the $U(1)$ broken phase and the unitary gauge has been chosen; as a consequence, this field has its own kinetic term and does not mix, as far as only bilinear terms are considered, with the gauge-field part of the action.

In [15], the field propagators related to the Lagrangian (3) were properly evaluated and taken as starting point to analyze the consistency of this planar model, which has been revealed to be totally causal and unitary for both timelike and spacelike backgrounds. Indeed, no problem concerning causality and unitarity was met with.

3 Wave equations for potentials and field strengths

We now go on writing the extended wave equations which govern the behavior for the potentials components and field strengths of the scalar electrodynamics stated in

[1] Here one has adopted the following metric conventions: $g_{\mu\nu} = (+,-,-,-)$ in $D = 1+3$, and $g_{\mu\nu} = (+,-,-)$ in $D = 1+2$.

the Lagrangian (3), from which there follow two Euler–Lagrangian equations of motion:

$$\partial_\nu F^{\mu\nu} = s\varepsilon^{\mu\nu\rho}\partial_\nu A_\rho + \varepsilon^{\mu\nu\rho}v_\nu\partial_\rho\varphi + M_A^2 A^\mu - J^\mu, \quad (4)$$

$$(\Box + M_A^2)\varphi = -\epsilon_{\mu\nu k}v^\mu\partial^\nu A^k - J, \quad (5)$$

which lead to the extended Maxwell equations:

$$\boldsymbol{\nabla}\times\boldsymbol{E} + \partial_t B = 0, \quad (6)$$

$$\partial_t\boldsymbol{E} - \nabla^* B = -\boldsymbol{j} - s\boldsymbol{E}^* - (\boldsymbol{v}^*\partial_t\varphi + v_0\boldsymbol{\nabla}^*\varphi) + M_A^2\boldsymbol{A}, \quad (7)$$

$$\boldsymbol{\nabla}\cdot\boldsymbol{E} - sB = \rho - M_A^2 A_0 + \boldsymbol{v}\times\boldsymbol{\nabla}\varphi, \quad (8)$$

$$(\Box + M_A^2)\varphi = v_0\boldsymbol{\nabla}\times\boldsymbol{A} - \boldsymbol{v}\times\boldsymbol{E} - J. \quad (9)$$

The first of these equations is the non-covariant form of the Bianchi identity ($\partial_\mu F^{\mu *} = 0$)[2]. The equation of motion (4) yields the two inhomogeneous ones, while (5) leads to the latter one. From such equations, one readily determines the mass dimension of the field strengths, namely $[E] = [B] = 3/2$. The original four-dimensional Lorentz breaking model is gauge invariant [1], a property transferred also to the planar model. It may be directly demonstrated from (4); one easily obtains $\partial_\mu J^\mu = -\varepsilon^{\mu\nu\rho}\partial_\mu v_\nu\partial_\rho\varphi$. Whenever v^μ is constant or has a null rotational ($\varepsilon^{\mu\nu\rho}\partial_\mu v_\nu = 0$), this equation leads to the conventional current-conservation law, $\partial_\mu J^\mu = 0$, consistent with gauge invariance.

From a pure algebraic manipulation of the Maxwell equations, one finds that the fields B, $\boldsymbol{E}$, satisfy second-order inhomogeneous wave equations:

$$(\Box + s^2 + M_A^2)B = -s\rho + \boldsymbol{\nabla}\times\boldsymbol{j} + sM_A^2 A_0 - s\boldsymbol{v}\times\nabla\varphi - \partial_t(\nabla\varphi)\times\boldsymbol{v}^* - v_0\nabla^2\varphi, \quad (10)$$

$$(\Box + s^2 + M_A^2)\boldsymbol{E} = -\boldsymbol{\nabla}\rho - \partial_t\boldsymbol{j} + s\boldsymbol{j}^* - \boldsymbol{\nabla}(\boldsymbol{v}\times\boldsymbol{\nabla}\boldsymbol{\varphi}) - s\boldsymbol{v}(\partial_t\varphi) - sv_0\boldsymbol{\nabla}\varphi - sM_A^2\boldsymbol{A}^* - \boldsymbol{v}^*\partial_t^2\varphi + v_0\boldsymbol{\nabla}^*(\partial_t\varphi). \quad (11)$$

Similarly to the classical MCS model, the potential components $(A_0, \boldsymbol{A})$ obey fourth-order wave inhomogeneous equations:

$$\left[\Box(\Box + s^2 + 2M_A^2) + M_A^2\right]A_0 = \left(\Box + M_A^2\right)[\rho + (\boldsymbol{v}\times\boldsymbol{\nabla}\boldsymbol{\varphi})] + s(\partial_t\boldsymbol{\nabla}\boldsymbol{\varphi})\times\boldsymbol{v}^* + s\boldsymbol{\nabla}\times\boldsymbol{j} - sv_0\nabla^2\varphi, \quad (12)$$

$$\left[\Box(\Box + s^2 + 2M_A^2) + M_A^2\right]\boldsymbol{A} = \left(\Box + M_A^2\right)(\boldsymbol{j} + \boldsymbol{v}\partial_t\varphi + v_0\boldsymbol{\nabla}^*\varphi) - s\boldsymbol{\nabla}^*\rho - s\partial_t\boldsymbol{j}^* + s\boldsymbol{v}\left(\partial_t^2\varphi\right) - sv_0\boldsymbol{\nabla}(\partial_t\varphi) - s\left(\boldsymbol{\nabla}(\boldsymbol{v}\times\boldsymbol{\nabla}\boldsymbol{\varphi})\right)^*, \quad (13)$$

[2] In $D = 1+2$ the dual tensor, defined as $F^{\mu *} = \frac{1}{2}\epsilon^{\mu\nu\alpha}F_{\nu\alpha}$, is a 3-vector given by $F^{\mu *} = (B, -\boldsymbol{E}^*)$. Here one adopts the following convention: $\epsilon_{012} = \epsilon^{012} = \epsilon_{12} = \epsilon^{12} = 1$. The symbol (*) designates the dual of a vector; it transforms an *arbitrary* 2-vector $\mathbf{A} = (A_x, A_y)$ in the form $\mathbf{A}^* = (A_y, -A_x)$.

It should be pointed out that the complexity of the inhomogeneous sector is directly related to the presence of the background 3-vector in the Lagrangian (3). In the absence of the background ($v^\mu \longrightarrow 0$), it is useful to verify that the wave equations (10), (11), (12) and (13) reduce to their classical usual MCS-Proca form:

$$\left[\Box(\Box + s^2 + 2M_A^2) + M_A^4\right]A_0 = \left(\Box + M_A^2\right)\rho + s\boldsymbol{\nabla}\times\boldsymbol{j}, \quad (14)$$

$$\left[\Box(\Box + s^2 + 2M_A^2) + M_A^4\right]\boldsymbol{A} = \left(\Box + M_A^2\right)\boldsymbol{j} - s\boldsymbol{\nabla}^*\rho - s\partial_t\boldsymbol{j}^*, \quad (15)$$

$$[\Box + s^2 + M_A^2]\boldsymbol{E} = -\boldsymbol{\nabla}\rho - \partial_t\boldsymbol{j} + s\boldsymbol{j}^* - sM_A^2\boldsymbol{A}^*, \quad (16)$$

$$[\Box + s^2 + M_A^2]B = -s\rho + \boldsymbol{\nabla}\times\boldsymbol{j} + sM_A^2 A_0. \quad (17)$$

For a static point-like charge distribution, the wave equations above have the following solutions:

$$A_0(r) = (e/2\pi)\,[c_+K_0(m_+r) + c_-K_0(m_-r)], \quad (18)$$

$$\boldsymbol{A}(r) = -(e/2\pi)\,c[m_+K_1(m_+r) - m_-K_1(m_-r)]\hat{r}^*, \quad (19)$$

$$\boldsymbol{E} = -(e/2\pi) \times [c_+m_+K_1(m_+r) + c_-m_-K_1(m_-r)]\hat{r}; \quad (20)$$

$$B(r) = -(e/2\pi)\,c[m_+^2K_0(m_+r) - m_-^2K_0(m_-r)], \quad (21)$$

with

$$c_\pm = \frac{1}{2}\left[1 \pm \frac{s}{\sqrt{s^2 + 4M_A^2}}\right], c = \frac{1}{\sqrt{s^2 + 4M_A^2}}, \quad (22)$$

$$m_\pm^2 = \frac{1}{2}\left[(s^2 + 2M_A^2) \pm s\sqrt{s^2 + 4M_A^2}\right]. \quad (23)$$

Near the origin these solutions behave as $A_0(r) \to -(e/2\pi)\ln r$, $\boldsymbol{A}(r) \to 0, \boldsymbol{E} \to (e/2\pi)\hat{r}/r$, $B(r) \to (e/2\pi)\,s\ln r$. Far from the origin, all these solutions vanish according to the asymptotic exponentially-decaying behavior of the Bessel functions. The solutions above will be used as a reference to help the identification of the contributions stemming from the presence of the background to the MCS-Proca electrodynamics stated in (3).

4 Solutions for the scalar potential and electric field in the static limit

In this section, we focus on the solutions for the scalar potential and electric field for a static point-like charge for the case of both timelike and spacelike Lorentz violating backgrounds. These solutions are worked out from the differential equations (9) and (12), which (in the static limit) become a coupled system of two differential equations.

4.1 The external vector is purely timelike: $v^\mu = (v_0, 0)$

In the case of a static configuration, (9) and (12) are reduced to the form

$$[\nabla^2(\nabla^2 - s^2 - 2M_A^2) + M_A^4]A_0 + sv_0\nabla^2\varphi = -(\nabla^2 - M_A^2)\rho, \quad (24)$$

$$v_0(\nabla^2 - M_A^2)A_0 - s(\nabla^2 - M_A^2)\varphi = -v_0\rho, \quad (25)$$

which consist of a system of two coupled linear differential equations. It is possible to decouple these two equations to get the following ones:

$$[\nabla^2(\nabla^2 - s^2 - 2M_A^2) + M_A^4 + v_0^2\nabla^2](\nabla^2 - M_A^2)A_0 = -\left[(\nabla^2 - M_A^2)(\nabla^2 - M_A^2) + v_0^2\nabla^2\right]\rho, \quad (26)$$

$$s[\nabla^2(\nabla^2 - s^2 - 2M_A^2) + M_A^4 + v_0^2\nabla^2][\nabla^2 - M_A^2]\varphi = -v_0\{[\nabla^2(\nabla^2 - s^2 - 2M_A^2) + M_A^4] + v(\nabla^2 - M_A^2)(\nabla^2 - M_A^2)\}\rho. \quad (27)$$

In order to solve (26), one proposes a point-like charge-density distribution, $\rho(r) = e\delta(r)$, and a Fourier-transform representation for the scalar potential, $A_0(r) = \frac{1}{(2\pi)^2}\int \mathrm{d}^2\boldsymbol{k}\mathrm{e}^{\mathrm{i}\boldsymbol{k}.\boldsymbol{r}}\widetilde{A}_0(k)$, so that there follows a Bessel K_0 solution:

$$A_0(r) = \frac{e}{(2\pi)}\left[\left(A_+ + v_0^2B_+\right)K_0\left(M_+r\right) + \left(A_- + v_0^2B_-\right)K_0\left(M_-r\right) - v_0^2\left(B_+ + B_-\right)K_0\left(M_Ar\right)\right], \quad (28)$$

where the involved constants are given below:

$$A_\pm = \frac{1}{2}\left[1 \pm \frac{(s^2 - v_0^2)}{\sqrt{(s^2 - v_0^2)(s^2 - v_0^2 + 4M_A^2)}}\right], \quad (29)$$

$$B_\pm = \left[\frac{2T_\pm}{(s^2 - v_0^2) \pm \sqrt{(s^2 - v_0^2)(s^2 - v_0^2 + 4M_A^2)}}\right], \quad (30)$$

$$T_\pm = \frac{1}{2}\left[1 \pm \frac{(s^2 - v_0^2 + 2M_A^2)}{\sqrt{(s^2 - v_0^2)(s^2 - v_0^2 + 4M_A^2)}}\right], \quad (31)$$

$$M_\pm^2 = \frac{1}{2}\left[(s^2 - v_0^2 + 2M_A^2) \pm \sqrt{(s^2 - v_0^2)(s^2 - v_0^2 + 4M_A^2)}\right]. \quad (32)$$

The electric field, derived from (28), is given simply by

$$\boldsymbol{E}(r) = -\frac{e}{(2\pi)}\left[-\left(A_+ + v_0^2B_+\right)M_+K_1\left(M_+r\right) - \left(A_- + v_0^2B_-\right)M_-K_1\left(M_-r\right) + v_0^2\left(B_+ + B_-\right)M_AK_1\left(M_Ar\right)\right]\hat{r}. \quad (33)$$

Both the electric field and scalar potential expressions present nearly the same functional behavior as the corresponding MCS-Proca, given by (18) and (20), when $v_0/s \ll 1$ or $M_A/s \sim 1$, as it shall be explained below.

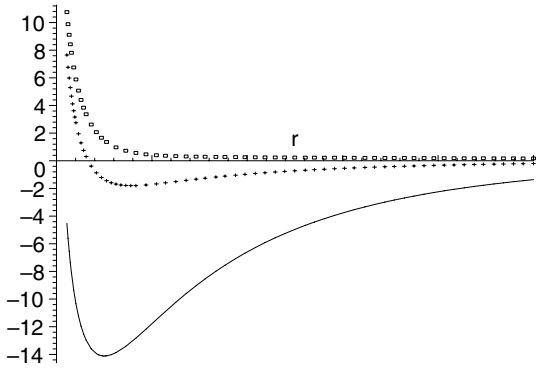

Fig. 1. Simultaneous plot of the pure MCS-Proca potential (box dotted line) for $s = 20, M_A = 2$; the scalar potential (circle dotted line) for $s = 20, M_A = 2, v_0 = 8$; the scalar potential for $s = 20, M_A = 2, v_0 = 15$ (continuous line)

The presence of the background is not decisive to determine qualitative modifications in their form both near and far from the origin. Indeed, in the limit of short distances ($r \ll 1$), the scalar potential (28) exhibits a purely logarithmic behavior, whereas the electric field (33) goes as a $1/r$ function,

$$A_0(r) = -\left(\frac{e}{2\pi}\right)\ln r, \qquad \boldsymbol{E}(r) = -\left(\frac{e}{2\pi}\right)\frac{1}{r}\hat{r}, \quad (34)$$

which reveals the repulsive character of (28) near the origin. It is interesting to remark that, in this limit, all the background corrections drop out, and do not lead to modifications to the MCS-Proca behavior near the origin. Far from the origin ($r \to \infty$), both the scalar potential and electric fields decay exponentially, showing an entirely screened behavior.

In a general sense, the background only seems to promote a damping in the screening of the solutions, increasing then their range. The smaller the factors $M_\pm$ are, the larger is the range. As far as $M_\pm^2 < m_\pm^2$, the range of these new solutions is larger than the MCS-Proca ones corresponding with them. Despite the functional similarity between the potentials (18) and (28), they may differ substantially in two clear situations:
(i) the Proca mass is small in comparison with the other mass parameters (s, M_+, M_-) of this solution, which turns the term $K_0(M_Ar)$ dominant and reverses the behavior of the scalar potential;
(ii) the modulus of v_0 is near the topological mass ($v_0/s \lesssim 1$), in which regime the influence of the background upon the solutions is maximal. The graphs in Figs. 1 and 2 illustrate these cases.

In Fig. 1 are shown three curves for a small value of the Proca mass ($M_A = 2$). One then verifies that the closer v_0 is from the s value (in this case $s = 20$), the bigger the deviation from the pure MCS-Proca behavior, as illustrated by the continuous curve. As the value of v_0 decreases, the scalar potential tends to the MCS-Proca behavior, as shown by the intermediate cross dotted line. For $v_0 = 0$, we obviously recover the pure MCS-Proca behavior, depicted by the box dotted line. The scalar potential

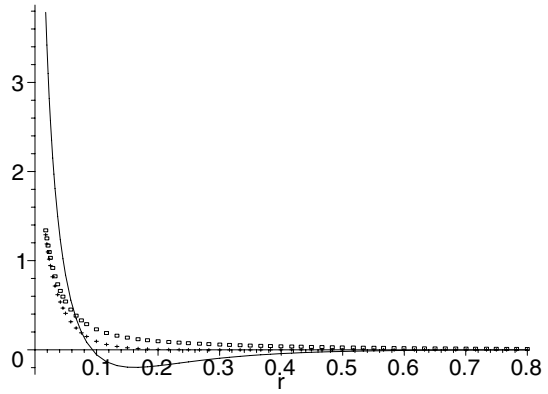

Fig. 2. Box dotted line: plot of the pure MCS-Proca potential for $s = 20, M_A = 8$; Cross dotted line: plot of the scalar potential for $s = 20, M_A = 8, v_0 = 8$; Continuous line: plot of the scalar potential for $s = 20, M_A = 8, v_0 = 17$

is negative in some radial extent due to the role played by the term $-K_0(M_A r)$, which becomes dominant over the $K_0(M_\pm r)$ terms for $M_A \ll M_\pm$. Hence, the attractiveness here observed is ascribed to the smallness of the ratio M_A/s. In Fig. 2, the same kind of simultaneous plot is displayed for a larger value of M_A, from where one notes that the deviations from the MCS-Proca behavior are strongly attenuated whenever the ratio M_A/s increases.

Both Figs. 1 and 2 show that the scalar potential is always repulsive near the origin and decays exponentially for large distances. Its behavior is very similar to the MCS-Proca one in the cases in which $v_0/s \ll 1$ or $M_A/s \sim 1$, but deviates substantially from it in the case one has $M_A \ll M_\pm$ or $v_0/s \lesssim 1$, for which one observes a potential that becomes attractive at intermediary distances. As a final point, it is important to remark that in the limit of a vanishing background ($v_0 \longrightarrow 0$), one trivially recovers the MCS-Proca solutions, since $A_\pm \to c_\pm$ in this situation.

4.2 The external vector is purely spacelike: $v^\mu = (0, \mathbf{v})$

In this case, one should consider (9) and (12), which in the static regime are written in the form

$$[\nabla^2(\nabla^2 - s^2 - 2M_A^2) + M_A^4]A_0 + \left(\nabla^2 - M_A^2\right)(\boldsymbol{v} \times \boldsymbol{\nabla\varphi}) = -(\nabla^2 - M_A^2)\rho, \quad (35)$$

$$(\boldsymbol{v} \times \boldsymbol{\nabla})A_0 + (\nabla^2 - M_A^2)\varphi = 0, \quad (36)$$

Decoupling these equations, one attains

$$[\nabla^2(\nabla^2 - s^2 - 2M_A^2) + M_A^4 - (\boldsymbol{v}^* \cdot \boldsymbol{\nabla})(\boldsymbol{v}^* \cdot \boldsymbol{\nabla})]A_0 = -(\nabla^2 - M_A^2)\rho, \quad (37)$$

$$[\nabla^2(\nabla^2 - s^2 - 2M_A^2) + M_A^4 - (\boldsymbol{v}^* \cdot \boldsymbol{\nabla})(\boldsymbol{v}^* \cdot \boldsymbol{\nabla})]\varphi = -(\boldsymbol{v}^* \cdot \boldsymbol{\nabla})\rho. \quad (38)$$

Starting from a point-like charge-density distribution, $\rho(r) = e\delta(r)$, and proposing again a Fourier-transform representation for the scalar potential, the solution will be given by the general the integral expression:

$$A_0(r) = \left(\frac{e}{(2\pi)^2} \int_0^\infty \frac{\mathbf{k}\mathrm{d}\mathbf{k}}{\left[\mathbf{k}^2 + R_+^2\right]} \int_0^{2\pi} P_+ \mathrm{e}^{ikr\cos\varphi} \mathrm{d}\varphi - \int_0^\infty \frac{\mathbf{k}\mathrm{d}\mathbf{k}}{\left[\mathbf{k}^2 + R_-^2\right]} \int_0^{2\pi} P_- \mathrm{e}^{ikr\cos\varphi} \mathrm{d}\varphi \right), \quad (39)$$

where

$$P_\pm = \frac{1}{2} \times \left[1 \pm \frac{(s^2 + v^2\sin^2\alpha)}{\sqrt{(s^2 + v^2\sin^2\alpha)(s^2 + v^2\sin^2\alpha + 4M_A^2)}} \right], \quad (40)$$

$$R_\pm^2 = \frac{1}{2}\left[(s^2 + 2M_A^2 + v^2\sin^2\alpha) \pm \sqrt{(s^2 + v^2\sin^2\alpha)(s^2 + 4M_A^2 + v^2\sin^2\alpha)} \right], \quad (41)$$

and α is the angle defined by the relation $\cos\alpha = \boldsymbol{v}\cdot\boldsymbol{k}/vk$, that is, the angle determined by the external background ($\boldsymbol{v}$) and transfer momentum ($\boldsymbol{k}$). The fact the constants $P_\pm, R_\pm$ depend on the angle variable (α) implies that the integrations above cannot be exactly solved. An exact result was not found for these integrations, but a sensible approximation can be performed in order to solve them algebraically. Indeed, considering the condition $s^2 \gg v^2$, some approximations are necessary so that the integration indicated becomes feasible. In this regime, one has

$$P_\pm \simeq \frac{1}{2}[1 \pm s/\gamma \pm \left(2M_A^2 v^2/s\gamma^3\right)\sin^2\alpha], \quad (42)$$

$$\frac{1}{\left[\mathbf{k}^2 + R_\pm^2\right]} \simeq \frac{1}{\left[\mathbf{k}^2 + m_\pm^2\right]} \mp \frac{m_\pm^2}{s\gamma} \frac{v^2\sin^2\alpha}{\left[\mathbf{k}^2 + m_\pm^2\right]^2}, \quad (43)$$

with $m_\pm^2 = \left[s^2 + 2M_A^2 \pm s\gamma\right]/2$, and $\gamma = \sqrt{s^2 + 4M_A^2}$. It should be remarked that the factors $m_\pm^2$ are exactly the ones that appear in the MCS-Proca solutions, given by (23). Here, one considers as well the angle between $\boldsymbol{v}$ and $\boldsymbol{r}$, given by $\cos\beta = \boldsymbol{v}\cdot\boldsymbol{r}/vr$, where $\beta = cte$. While the background vector, $\boldsymbol{v}$, sets up a fixed direction in space, the coordinate vector, $\boldsymbol{r}$, defines the position where the potentials are to be measured; so, β is the (fixed) angle that indicates the directional dependence of the fields in relation to the background direction. Being confined to the plane, these angles satisfy a simple relation: $\alpha = \varphi - \beta$, which allows for the evaluation of the angular integration on the φ variable, based on the following expression: $\sin^2\alpha = \cos^2\beta - (\cos 2\beta)\cos^2\varphi + c_3 \sin 2\varphi$. Considering all that, one has

$$\int_0^{2\pi} \left[P_- \mathrm{e}^{ikr\cos\varphi}\right] \mathrm{d}\varphi \simeq \frac{(2\pi)}{2}\left[\left(1 - s/\gamma - \epsilon\sin^2\beta\right) J_0(\mathbf{k}r) + \epsilon\cos 2\beta J_1(\mathbf{k}r)/\left(\mathbf{k}r\right)\right], \quad (44)$$

$$\int_0^{2\pi}\left[P_+ \mathrm{e}^{\mathrm{i}kr\cos\varphi}\right]\mathrm{d}\varphi \simeq \frac{(2\pi)}{2}\left[\left(1+s/\gamma+\epsilon\sin^2\beta\right)J_0(\mathbf{k}r) - \epsilon\cos 2\beta J_1(\mathbf{k}r)/\left(\mathbf{k}r\right)\right], \quad (45)$$

with $\epsilon = 2M_A^2 v^2/s\gamma^3$. However, the task is not complete yet. In order to solve the integration in $\mathrm{d}k$, it is essential to notice that the terms $R_\pm^2$, given in (41), are also dependent on the angle variable, requiring the use of another suitable approximation, given in (43). Taking into account the above angular integrations, one then carries out the k-integrations, arriving (at first order in v^2/s^2) at a lengthy expression for the scalar potential, namely

$$A_0(r) = \frac{e}{2(2\pi)}\Big\{\delta_+ K_0(m_+r) + \delta_- K_0(m_-r) - \sigma_+(r)K_1(m_+r) + \sigma_-(r)K_1(m_-r)\Big\}, \quad (46)$$

where

$$\delta_\pm = \left[1 \pm s/\gamma \pm \frac{v^2}{2s\gamma^3}(\gamma^2 \pm s\gamma - 4m_+^2\sin^2\beta)\right];$$
$$\sigma_\pm(r) = v^2\left[-\frac{2m_\pm}{s\gamma^3}\frac{\cos 2\beta}{r} + \frac{m_\pm\left(1\pm s/\gamma\right)\sin^2\beta}{2s\gamma}r\right].$$

In this expression, one notes a clear dependence of the potential on the angle β, which is an unequivocal sign of anisotropy determined by the ubiquity of the background vector in the system.

The electric field can be obtained in a straightforward way from (46); it looks as follows:

$$\boldsymbol{E}(r) = -\frac{e}{2(2\pi)}\left\{-m_+\left[\delta_+ - \frac{4v^2\cos 2\beta}{s\gamma^3 r^2}\right]K_1(m_+r) - m_-\left[\delta_- - \frac{4v^2\cos 2\beta}{s\gamma^3 r^2}\right]K_1(m_-r) + m_+\sigma_+ K_0(m_+r) - m_-\sigma_- K_0(m_-r)\right\}\hat{r}. \quad (47)$$

Near the origin, the short-distance potential behaves like as a genuine logarithmic function, whereas the electric field goes as a $1/r$ function:

$$A_0(r) = -\frac{e}{(2\pi)}\left[1+\frac{v^2}{2\gamma^2}(1-\cos 2\beta)\right]\ln r,$$
$$\boldsymbol{E}(r) = -\frac{e}{(2\pi)}\left[1+\frac{v^2}{2\gamma^2}(1-\cos 2\beta)\right]\frac{\hat{r}}{r}. \quad (48)$$

Such expressions reveal that the scalar potential is always repulsive at the origin. The presence of the anisotropy factor is not able to revert this behavior, since $v^2 \ll s^2$. Far away from the origin, the long-range potential vanishes according to the behavior of the Bessel functions, namely $A_0(r) \to 0$, $\boldsymbol{E}(r) \to 0$. This result shows that these solutions decay rapidly as $r \to \infty$, revealing a strong screening as already observed in the pure timelike case.

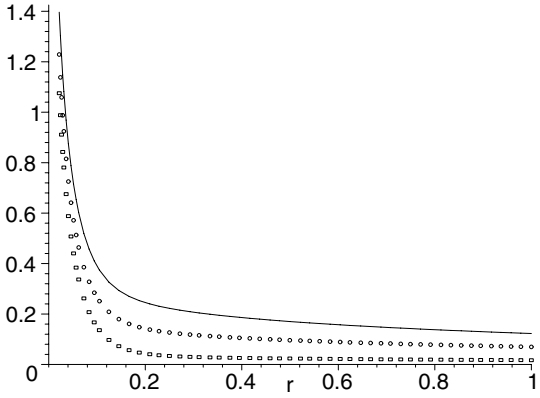

Fig. 3. Simultaneous plot of the MCS-Proca scalar potential (box dotted curve), scalar potential for $\beta = \pi/4$ (circle dotted curve), scalar potential for $\beta = \pi/2$ (continuous curve). The common parameter values are $s = 20, M_A = 2, v = 5$

The graphics in Fig. 3 displays the behavior of the scalar potential compared with the MCS-Proca one. It should be reported that the scalar potential has shown to be always positive for all the values of parameters adopted. This last illustration shows that the deviations from the MCS-Proca behavior are small, a consequence of the approximation $v^2/s^2 \ll 1$, which does not allow one to probe the form of the scalar potential for larger values of the background.

It can be easily observed that in the absence of the background, $\boldsymbol{v} = 0$, the scalar potential and the electric field are reduced to the corresponding MCS-Proca ones: $A_0(r) = e/2(2\pi)[(1+s/\gamma)K_0(m_+r) + (1-s/\gamma)K_0(m_-r)]$, $\boldsymbol{E}(r) = -e/2(2\pi)[(1+s/\gamma)m_+K_0(m_+r) + (1-s/\gamma)m_-K_0(m_-r)]\hat{r}$, which are the solutions given in (18) and (20). Here, the effect of the background vector, $\boldsymbol{v}$, appears more clearly on the field solutions. As compared with the MCS-Proca fields (B and $\boldsymbol{E}$), there arise supplementary terms, depending on the background and on the angle β, responsible for the spatial anisotropy.

As for the solution for the scalar field in the case of a purely spacelike background, it can be obtained starting from (38), which, according to the procedure adopted so far, yields the following integral expression:

$$\varphi(r) = \frac{e}{(2\pi)^2}\left(\boldsymbol{v}^*\cdot\boldsymbol{\nabla}\right) \times\left[\int_0^\infty \frac{\mathbf{k}\mathrm{d}\mathbf{k}}{\left[\mathbf{k}^2+R_+^2\right]}\int_0^{2\pi} Q\mathrm{e}^{\mathrm{i}kr\cos\varphi}\mathrm{d}\varphi - \int_0^\infty \frac{\mathbf{k}\mathrm{d}\mathbf{k}}{\left[\mathbf{k}^2+R_-^2\right]}\int_0^{2\pi} Q\mathrm{e}^{\mathrm{i}kr\cos\varphi}\mathrm{d}\varphi\right], \quad (49)$$

where $Q = \left[(s^2+v^2\sin^2\alpha)(s^2+4M_A^2+v^2\sin^2\alpha)\right]^{-1/2}$. Making use of (43) and the suitable approximation, $Q \simeq 1/(s\gamma) - (s^2+2M_A^2)v^2\sin^2\alpha/(s\gamma)^3$, a lengthy solution may be attained for the scalar field after a boring calculation, namely

$$\varphi(r) = -\frac{e}{(2\pi)}\Big\{m_+\varrho_+(r)K_1(m_+r) - m_-\varrho_-(r)K_1(m_-r) - \varsigma_+(r)K_0(m_+r) + \varsigma_-(r)K_0(m_-r)\Big\}\left(\boldsymbol{v}^*\cdot\hat{r}\right), \quad (50)$$

where

$$\varrho_\pm(r) = \left[\frac{1}{s\gamma} - \frac{2m_\pm^2}{(s\gamma)^3}v^2\sin^2\beta \pm \frac{v^2}{2\,(s\gamma)^2} + \frac{4v^2\cos 2\beta}{(s\gamma)^3}\frac{1}{r^2}\right],$$
$$\varsigma_\pm(r) = \frac{m_+^2v^2}{2(s\gamma)^2}\left(\pm r\sin^2\beta - \frac{4\cos 2\beta}{(s\gamma)}\frac{1}{r}\right).$$

Near the origin, this solution behaves as $\varphi(r) \to -e/(2\pi)[1/(s\gamma)^2]\,(1/r)\left(\boldsymbol{v}^*\cdot\hat{r}\right)$, implying an attractive character in this limit. Concerning the asymptotic behavior, the scalar solution vanishes exponentially.

5 Solutions for the vector potential and the magnetic field in the static limit

In this section, we aim at constructing the solutions for the vector potential and magnetic field for a point-like static charge for both a timelike and spacelike Lorentz violating backgrounds. These solutions are achieved from the differential equations (9) and (13), which in the static limit constitute a coupled system of two differential equations.

5.1 The external vector is purely timelike: $v^\mu = (v_0, 0)$

Starting from (5) and (13), one writes the following system in the static limit:

$$[\nabla^2(\nabla^2 - s^2 - 2M_A^2) + M_A^4]\boldsymbol{A} + v_0\left(\nabla^2 - M_A^2\right)(\nabla^*\varphi) = -s\boldsymbol{\nabla}^*\rho,$$
$$v_0\nabla\times\boldsymbol{A} + \left(\nabla^2 - M_A^2\right)\varphi = 0,$$

which may be decoupled in two equations for the vector potential and the scalar field:

$$[\nabla^2(\nabla^2 - s^2 - 2M_A^2) + M_A^4]\boldsymbol{A} = -s\boldsymbol{\nabla}^*\rho, \quad (51)$$
$$[\nabla^2(\nabla^2 - s^2 - 2M_A^2) + M_A^4]\left(\nabla^2 - M_A^2\right)\varphi = sv_0\nabla^2\rho. \quad (52)$$

Proposing a Fourier-transform representation for the vector potential, $\boldsymbol{A}(r) = \frac{1}{(2\pi)^2}\int \mathrm{d}^2\boldsymbol{k}\mathrm{e}^{\mathrm{i}\boldsymbol{k}.\boldsymbol{r}}\widetilde{A}(k)$, it turns out to be

$$\boldsymbol{A}(r) = -\frac{es}{(2\pi)}C\left[M_+K_1\left(M_+r\right) - M_-K_1\left(M_-r\right)\right]\hat{r}^*, \quad (53)$$

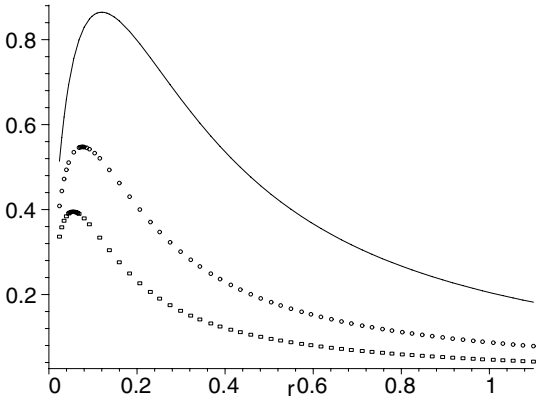

Fig. 4. Simultaneous plot for the MCS-Proca vector potential (box dotted line), vector potential for $v_0 = 14$ (circle dotted line) and vector potential for $v_0 = 18$ (continuous line), with $s = 20, M_A = 2$

where $C = 1/\sqrt{(s^2 - v_0^2)(s^2 - v_0^2 + 4M_A^2)}$, and the terms $M_\pm^2$ are defined in (32). The magnetic field, $B = \boldsymbol{\nabla}\times\boldsymbol{A}$, stems directly from the equation above in the form

$$B(r) = -\frac{es}{(2\pi)}C\left[M_+^2K_0\left(M_+r\right) - M_-^2K_0\left(M_-r\right)\right].$$

Comparing these solutions with the MCS-Proca counterparts, one then notices that the background does not impose any functional modification. Its role is limited to yielding an increasing of the associated range, which can be observed in Fig. 4.

It is simple to notice that the solutions here attained for $\mathbf{A}$ and B present the same behavior of the MCS-Proca case both near and far from the origin. Indeed, for $r \to 0$, the vector potential vanishes ($\mathbf{A} \to 0$), whereas the magnetic field behaves like a pure logarithmic function:

$$B(r) \to \left(-\frac{es}{2\pi}\right)\ln r,$$

in much the same way as the MCS-Proca behavior. Far from the origin, both these fields vanish exponentially.

In Fig. 4 is shown for illustration a comparison between the MCS-Proca vector potential and the one given by (53), which clarifies the role of the background: the larger is v_0, the larger is the deviation from the MCS-Proca behavior (the potential becomes more positively pronounced).

In this section, it is still possible to derive a solution for the scalar field in the case of a purely timelike background, which stems from (52). This solution is easily attained following the usual procedure here adopted:

$$\varphi(r) = \frac{e}{(2\pi)}\,(sv_0) \times \left[B_+K_0\left(M_+r\right) + B_-K_0\left(M_-r\right) - (B_+ + B_-)K_0\left(M_Ar\right)\right],$$

where the coefficients $B_\pm$ are given in (30) and (31). Near the origin this solution vanishes identically, that is $\varphi(r) \to 0$. Far from the origin it vanishes exponentially according to the Bessel-like asymptotic behavior.

5.2 The external vector is purely spacelike: $v^\mu = (0, \mathbf{v})$

Starting from (9) and (13), one attains

$$[\nabla^2(\nabla^2 - s^2 - 2M_A^2) + M_A^4]\boldsymbol{A} - s\boldsymbol{\nabla}^*(\boldsymbol{v}\cdot\boldsymbol{\nabla}^*\varphi) = -s\boldsymbol{\nabla}^*\rho, \quad (54)$$

$$[(\boldsymbol{v}^*\cdot\boldsymbol{\nabla})\nabla\times + M_A^2\boldsymbol{v}\cdot]\boldsymbol{A} - s\left(\nabla^2 - M_A^2\right)\varphi = 0, \quad (55)$$

which can be decoupled in the two following equations:

$$\left[[\nabla^2(\nabla^2 - s^2 - 2M_A^2) + M_A^4] + (\boldsymbol{v}\cdot\boldsymbol{\nabla}^*)(\boldsymbol{v}\cdot\boldsymbol{\nabla}^*)\right]\boldsymbol{A} = -s\boldsymbol{\nabla}^*\rho, \quad (56)$$

$$\left[[\nabla^2(\nabla^2 - s^2 - 2M_A^2) + M_A^4 + (\boldsymbol{v}\cdot\boldsymbol{\nabla}^*)(\boldsymbol{v}\cdot\boldsymbol{\nabla}^*)]\left(\nabla^2 - M_A^2\right)\right]\varphi = [(\boldsymbol{v}^*\cdot\boldsymbol{\nabla})\nabla\times + M_A^2\boldsymbol{v}\cdot]\nabla^*\rho. \quad (57)$$

The solution of (56) is given by the following integral expression:

$$\boldsymbol{A}(r) = -\frac{es}{(2\pi)^2}\boldsymbol{\nabla}^*\left[\int_0^\infty \frac{\mathbf{k}\mathrm{d}\mathbf{k}}{\left[\mathbf{k}^2 + R_+^2\right]}\int_0^{2\pi} D\mathrm{e}^{\mathrm{i}kr\cos\varphi}\mathrm{d}\varphi - \int_0^\infty \frac{\mathbf{k}\mathrm{d}\mathbf{k}}{\left[\mathbf{k}^2 + R_-^2\right]}\int_0^{2\pi} D\mathrm{e}^{\mathrm{i}kr\cos\varphi}\mathrm{d}\varphi\right], \quad (58)$$

where $D = 1/\sqrt{(s^2 + v^2\sin^2\alpha)(s^2 + v^2\sin^2\alpha + 4M_A^2)}$, and the factors $R_\pm^2$ are given by (41). In order to solve the integrations involved in this expression, one should use the approximation (43) supplemented by the following one:

$$D \simeq -\frac{1}{s\gamma} + \frac{\left(s^2 + 2M_A^2\right)}{(s\gamma)^3}v^2\sin^2\alpha,$$

Considering all that, we achieve again a lengthy result:

$$\boldsymbol{A}(r) = -\frac{es}{(2\pi)}\Big\{\chi_+(r)K_0(m_+r) + \chi_-(r)K_0(m_-r) + \omega_+(r)K_1(m_+r) + \omega_-(r)K_1(m_-r)\Big\}\hat{r}^*, \quad (59)$$

where

$$\chi_\pm(r) = -\frac{m_\pm v^2}{(s\gamma)^2}\left(\mp\frac{2m_\pm}{(s\gamma)}\frac{\cos 2\beta}{r} + \frac{m_\pm\sin^2\beta}{2}r\right), \quad (60)$$

$$\omega_\pm(r) = \mp m_\pm\left(-\frac{1}{s\gamma} + \frac{v^2}{(s\gamma)^3}\left(2m_\pm^2\sin^2\beta \mp \frac{s\gamma}{2}\right)\right) \pm \frac{4v^2m_+}{(s\gamma)^3}\frac{\cos 2\beta}{r^2}, \quad (61)$$

where the spatial anisotropy determined by the fixed background becomes manifest. Considering the behavior of the K_0, K_1 functions near the origin [$K_0(sr) \to -\ln r - \gamma_{\mathrm{Euler}} - \ln(s/2)$, $K_1(sr) \to 1/(sr) + sr(\ln r/2 + \ln(s/2)/2 + (1 - 2\gamma_{\mathrm{Euler}})/4$], it is possible to show (after some algebraic calculations) that the vector potential vanishes in this limit ($\boldsymbol{A}(r) \to 0$ for $r \to 0$). Far away from the origin, all the terms can be neglected, so that the vector potential also vanishes asymptotically. It is interesting to remark that the vector potential vanishes near and far from the origin for both time- and spacelike backgrounds, recovering the pure MCS-Proca behavior. This fact demonstrates that the background does not impose physical changes into this potential in these two limits.

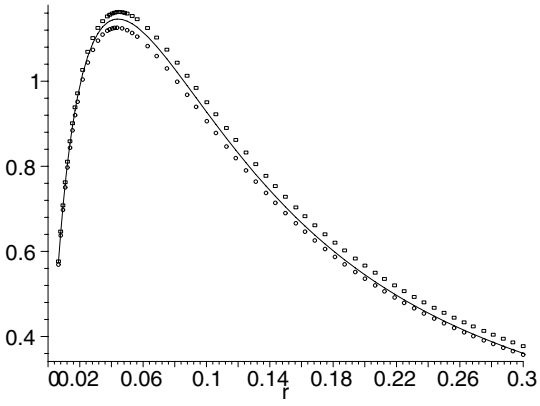

Fig. 5. Simultaneous plot for the MCS-Proca vector potential (box dotted line), vector potential for $\beta = \pi/3$ (circle dotted line) and vector potential for $\beta = \pi$ (continuous line), with $s = 24, M_A = 4, v = 8$

In Fig. 5, one illustrates the behavior of the vector potential compared to the MCS-Proca vector potential. One observes that the deviations from the MCS-Proca behavior are very small as a consequence of the approximation adopted, $(v/s)^2 \ll 1$. In this case, it is notorious that the background is unable to bring about expressive modifications even at the intermediary radial region. A similar conclusion follows from Fig. 3, which exhibits the behavior of the scalar potential (derived under the same approximation).

We can now finish by evaluating the magnetic field associated with this vector potential, which takes the form below:

$$B(r) = \frac{es}{(2\pi)}\Big\{\eta_+(r)K_0(m_+r) + \eta_-(r)K_0(m_-r) + \xi_+(r)K_1(m_+r) + \xi_-(r)K_1(m_-r)\Big\}, \quad (62)$$

where

$$\eta_\pm(r) = -\frac{m_\pm^2}{s\gamma} + \frac{2m_\pm^4v^2}{(s\gamma)^3}\sin^2\beta + \frac{m_\pm^2v^2}{2(s\gamma)^2}(\pm 1 - 2\sin^2\beta) \pm \frac{4m_\pm^2v^2}{(s\gamma)^3}\frac{\cos 2\beta}{r^2},$$

$$\xi_\pm(r) = \frac{m_\pm^3v^2\sin^2\beta}{2(s\gamma)^2}r \mp \frac{8m_\pm v^2}{(s\gamma)^3}\frac{\cos 2\beta}{r^3}$$

$$\mp \frac{2m_{\pm}^2 v^2}{(s\gamma)^3}\frac{\cos 2\beta}{r}.$$

Near the origin, this magnetic field recovers the MCS-Proca behavior [$B(r) \to \ln r$ for $r \to 0$], while it exponentially vanishes asymptotically.

6 Final remarks

Starting from a dimensionally reduced gauge invariant, but Lorentz and CPT violating planar model [15], derived from the Carroll–Field–Jackiw Abelian–Higgs model [9], we have studied the extended Maxwell equations (and the corresponding wave equations for the field strengths and potentials) stemming from this planar Lagrangian. While the field strengths satisfy second-order inhomogeneous wave equations, the potential components $(A_0, \boldsymbol{A})$ fulfill fourth-order wave equations, in a clear similarity to the usual behavior inherent to the pure MCS-Proca electrodynamics. As expected, this structural resemblance is also manifest in the solutions to these equations.

In the case of a purely timelike background, one has attained solutions for the potentials $(A_0, \boldsymbol{A})$ and fields $(B, \boldsymbol{E})$ that behave very similarly in some respects to the MCS-Proca counterparts. Specifically, the solutions worked out possess an identical behavior to the MCS-Proca counterpart near and far from the origin, revealing that the background does not affect the MCS-Proca solutions in both these limits. The qualitative differences induced by the background appear *at* an intermediary radial region, in which the solutions deviate from the MCS-Proca counterpart in a pronounced way in the case of a small Proca mass ($M_A/s \ll 1$) or a large background ($v_0 \lesssim s$). Another effect of the background is the increasing of the range of the solutions, also manifest in a more notorious way for $v_0 \lesssim s$. Once the purely timelike backgrounds allow for the attainment of exact algebraic solutions, the value of v_0 may be taken as close to the value of s as possible, which points out the role of the background. The graphs in Figs. 1 and 4 illustrate these conclusions. The MCS-Proca solutions are readily recovered whenever the background is supposed to vanish or is very small in comparison with the other mass parameters. A solution for the scalar field (φ) was also derived, exhibiting a similar structure to the scalar potential for both timelike and spacelike backgrounds.

In the pure spacelike case, the solutions may not be obtained exactly. In order to solve the angular integrations involved, some approximations were considered. In general, one regards the regime in which the Chern–Simons mass parameter is much larger than the background modulus ($s^2 \gg v^2$), so that the solutions derived are valid to the first order in v^2/s^2. Due to this approximation, there appear complex combinations of Bessel K_0 and K_1 functions as solutions for the potentials and field strengths. All these expressions depend on the angle β, which represents the dependence of the solutions on the 2-direction fixed by the background ($\boldsymbol{v}$). It must be stated that all these non-trivial solutions are reduced to the simple MCS-Proca solutions in case of a vanishing background. Analogously to the purely timelike case, the effect of the background on the scalar potential and vector potential disappears in the limits $r \to 0, r \to \infty$, in which they recover the correlated MCS-Proca behavior. It should be remarked that even at intermediary regions these solutions exhibit only small deviations from the MCS-Proca solutions, a direct consequence of the approximation adopted ($s^2 \gg v^2$), which prevents the investigation in a situation of a large background ($v_0 \lesssim s$). In order to properly analyze the solutions in this latter limit, it would be necessary to obtain exact algebraic solutions, valid for any value of the modulus of the background. In this case, one believes that the resulting solutions would exhibit remarkable deviations from the MCS-Proca counterparts, as observed in the purely timelike case. Concerning the scalar field, a solution was attained in much the same way as done for the potentials, exhibiting a similarly anisotropic structure. Finally, it should be pointed out that all solutions obtained as a result appear to be entirely shielded, a consequence of the Proca mass, which prevents the appearance of unescreened solutions (logarithmic ones), as it occurs in the case of the analogous MCS-Lorentz violating planar model solved in [14].

The solutions for the scalar potential of this work put in evidence the possibility of attaining an attractive behavior and the possible formation of bound states. Concerning an electron–electron interaction, this issue may be properly investigated by means of the interaction potential stemming from the evaluation of the Möller scattering amplitude. Such a calculation was already carried out in the context of Lorentz violating theories in three and four dimensions [17]. In the case of the planar model of [13], the Möller interaction potential obtained presents an asymptotic logarithmic behavior which represents an unreal physical interaction in a planar dimension. In the case of the present Abelian–Higgs Lorentz violating model, it is expected that such an evaluation yield a screened solution, suitable for describing a real interaction in condensed matter planar systems. This issue is now under investigation.

References

1. S.M. Carroll, G.B. Field, R. Jackiw, Phys. Rev. D **41**, 1231 (1990)
2. D. Colladay, V.A. Kostelecký, Phys. Rev. D **55**, 6760 (1997); **58**, 116002 (1998)
3. V.A. Kostelecky, S. Samuel, Phys. Rev. D **39**, 683 (1989); V.A. Kostelecky, R. Potting, Nucl. Phys. B **359**, 545 (1991); Phys. Lett. B **381**, 89 (1996); Phys. Rev. D **51**, 3923 (1995)
4. S.R. Coleman, S.L. Glashow, Phys. Rev. D **59**, 116008 (1999); V.A. Kostelecký, M. Mewes, Phys. Rev. Lett. **87**, 251304 (2001); Phys. Rev. D **66**, 056005 (2002)
5. R. Bluhm, A. Kostelecy, C. Lane, Phys. Rev. Lett. **84**, 1098 (2000); R. Bluhm, A. Kostelecy, Phys. Rev. Lett. **84**, 1381 (2000); R. Bluhm, A. Kostelecy, C. Lane, N. Russell, Phys. Rev. Lett. **88**, 090801 (2002); O. Gagnon,

G.D. Moore, Phys. Rev. D **70**, 065002 (2004); H. Mueller, Phys. Rev. D **71**, 045004 (2005); J.A. Lipa et al., Phys. Rev. Lett. **90**, 060403 (2003); P. Wolf et al., Phys. Rev. D **70**, 051902 (2004)
6. C. Adam, F.R. Klinkhamer, Nucl. Phys. B **607**, 247 (2001); Phys. Lett. B **513**, 245 (2001); V.A. Kostelecky, R. Lehnert, Phys. Rev. D **63**, 065008 (2001); A.A. Andrianov, R. Soldati, L. Sorbo, Phys. Rev. D **59**, 025002 (1999); R. Lehnert, Phys. Rev. D **68**, 085003 (2003); J. Math. Phys. **45**, 3399 (2004)
7. M. Goldhaber, V. Timble, J. Astrophys. Astron. **17**, 17 (1996); D. Hutsemékers, H. Lamy, Astron. Astrophys. **332**, 410 (1998); **367**, 381 (2001)
8. R. Jackiw, V.A. Kostelecký, Phys. Rev. Lett. **82**, 3572 (1999); J.M. Chung, B.K. Chung, Phys. Rev. D **63**, 105015 (2001); J.M. Chung, Phys. Rev. D **60**, 127901 (1999); M. Perez-Victoria, Phys. Rev. Lett. **83**, 2518 (1999); R. Jackiw, V.A. Kostelecky, Phys. Rev. Lett. **82**, 3572 (1999); G. Bonneau, Nucl. Phys. B **593**, 398 (2001); M. Perez-Victoria, JHEP **0104**, 032 (2001); A.P. Baêta Scarpelli et al., Phys. Rev. D **64**, 046013 (2001)
9. A.P. Baêta Scarpelli, H. Belich, J.L. Boldo, J.A. Helayël-Neto, Phys. Rev. D **67**, 085021 (2003)
10. H. Belich et al., Phys. Rev. D **68**, 065030 (2003); Nucl. Phys. B Suppl. **127**, 105 (2004)
11. R. Lehnert, R. Potting, Phys. Rev. Lett. **93**, 110402 (2004); Phys. Rev. D **70**, 125010 (2004)
12. C. Adam, F.R. Klinkhamer, Nucl. Phys. B **657**, 214 (2003)
13. H. Belich, M.M. Ferreira Jr., J.A. Helayël-Neto, M.T.D. Orlando, Phys. Rev. D 67, 125011 (2003); D **69**, 109903(E) (2004)
14. H. Belich, M.M. Ferreira Jr., J.A. Helayël-Neto, M.T.D. Orlando, Phys. Rev. D **68**, 025005 (2003)
15. H. Belich, M.M. Ferreira Jr., J.A. Helayël-Neto, Eur. Phys. J. C **38**, 511 (2005)
16. H. Belich, T. Costa-Soares, M.M. Ferreira Jr., J.A. Helayël-Neto, M.T.D. Orlando, hep-th/0407260
17. M.M. Ferreira Jr., Phys. Rev. D **70**, 045013 (2004); D **71**, 045003 (2005); B. Altschul, Phys. Rev. D **70**, 056005 (2004)